

Ministry of Higher Education
and Scientific Research



Journal of Kufa for Chemical Sciences

A refereed

Research Journal Chemical Sciences

Vol.2 No.8

Year 2022

ISSN 2077-2351

مجلة الكوفة لعلوم الكيمياء

Preparation and study photocatalytic properties of BiOX

(X= Cl, Br, I)

Batool K. Hashim, Zaki N. Kadhim

Chemistry Department, College of Science, University of Basrah, Basrah

zaki.kadhim@uobasrah.edu.iq, batool.hatim.sci@uobasrah.edu.iq

الخلاصة:

في الآونة الأخيرة ، اكتسبت مواد أكسي هاليد البزموت اهتمامًا متزايدًا إذ تُظهر صفة التحفيز الضوئي المحتملة لأن هياكلها ذات الطبقات الاستثنائية تمنحها خصائص فيزيائية كيميائية جذابة. حضرت مركبات (BiOX, X= Cl, Br, I) ، وقد استعملت عملية التحفيز الضوئي لإزالة صبغة الانديكو كارمين الملوثة لمياه الصرف الصناعي. حيث تم دراسة بعض العوامل المؤثرة على عملية الازالة منها تأثير كمية المحفز ، الدالة الحامضية ، درجة الحرارة و التركيز الابتدائي للصبغة. لقد تم دراسة جميع العوامل المؤثرة على ازالة صبغة الانديكو كارمين بوجود مصباح الأشعة فوق البنفسجية بطول موجي 245nm ثم دراسة الخصائص الترموديناميكية لامتنزاز الصبغة وإيجاد قيم الدوال الترموديناميكية (ΔH , ΔS , ΔG). تم تعيين ايزوثرمات الامتنزاز من خلال معادلتى لانكماير- فريندلخ حيث كان امتزاز الصبغة على سطح المركب (BiOCl, BiOI) خاضعة لمعادلة فريندلخ و(BiOBr) خاضعة لمعادلة لانكماير، تمت الدراسة الحركية لامتنزاز الصبغة بتطبيق معادلتى المرتبة الأولى والثانية الكاذبتين وبينت النتائج العملية ان حركية امتزاز الصبغة المستخدمة في الدراسة خاضعة لمعادلة المرتبة الثانية الكاذبة. تم تشخيص المركب بتقنيات الأشعة تحت الحمراء (FTIR)، حيود الأشعة السينية (XRD) و المسح الالكتروني (SEM).

Abstract:

Recently, bismuth oxyhalide materials have established more and more interest as shows potential photocatalysts because their exceptional layered structures give them with attractive physicochemical properties, and the photocatalysis process was used to remove the polluting indigo carmine dye from industrial wastewater. Where some factors affecting the treatment process were studied, including the effect of the amount of catalyst, pH, temperature and the initial concentration of the dye. All factors affecting the removal of indigo carmine dye in the presence of ultraviolet radiation lamp of wavelength 245 nm have been studied. Then study the thermodynamic properties of dye adsorption and find the values of thermodynamic functions (ΔH , ΔS , ΔG). The adsorption isotherms were determined by the Langumire-Freundlich equations, where the adsorption of the dye on the surface of the (BiOCl, BiOI) compounds was subject to freundlich equation, (BiOBr) was subject to langumire equation. The kinetics of dye adsorption was also studied by applying the pseudo first and second order equations, the

practical results shown that the adsorption kinetics of the dye used in the study is subject to the pseudo second order equation. The compound was identified by infrared (IR), X-ray diffraction (XRD) and scanning electron (SEM) techniques.

1. INTRODUCTION

Pollution environmental has become a major confront for the developing reigns and the developed world due to the industrial uprising, which on the one hand facilitates life and on the other hand wipe out the environment.

Textile, chemical, oil, and gas industries once a year launch billion of tons of harmful liquid waste to groundwater and upper environment, which unfavorably affects marine life, humans and plants^(1,2). Nowadays, there are many techniques that have been discovered to gather the problem of fast growth, the most common method used to eliminate pollutants involves the use of physical materials, chemical processes, biological and thermal techniques to remove commonly found organic and inorganic pollutants^(3,4). One of the many planned processes being developed for decontamination, biodegradation has established the most attention. In contrast, many organic materials, particularly that are toxic or heat-resistant, are highly resistant to biodegradation^(5,6). Consequently, after the finding of photocatalytic splitting of water by Fujishima and Honda⁽⁷⁾ in 1972, the researchers turned their point of junction toward semiconductor photocatalysis which proved very effective in the degradation of even those pollutants which are highly difficult to remove by the other means. Compare with the traditional oxidation process, the photocatalysis has considerable advantages, for example, they can be used to degrade the dyes and chemicals totally to CO₂ and H₂O and are also accommodating in the degradation of very stable compounds which cannot be easily degraded by the other processes, also they can work well at ambient temperature and pressure conditions, and they do not need any extraordinary supply of oxygen. Other advantage of the photocatalysis is that it is a cheap process as compared to the other oxidation process having no waste disposal problems⁽⁸⁾. Among many photocatalyst (BiOX, X= Cl, Br, I) used as a photocatalyst to elimination a lot of pollutants like dyes⁽⁹⁾, organic pollutants⁽¹⁰⁾. Clean and mixed bismuth oxyhalides with layered structures have confirmed outstanding photocatalytic activities⁽¹¹⁾ and offer a new family of promising photocatalysts. BiOX (X = Cl, Br, I), are cheap. Until now , many oxides containing bismuth (Bi) have high photocatalytic activity , such as Bi₂O₃⁽¹²⁾, Bi₂WO₆⁽¹³⁾. Due to the electron structure of Bi. Wherefore, the

photocatalytic activity is directly related to the mobility of the photogenerated charge carriers and the positions of the conduction band (CB) and valence band (VB) in the photocatalyst. In metal oxide photocatalysts, the VB is commonly composed of O 2p. Only, the VB of materials that contain element Bi mostly consists of O 2p and Bi 6s hybrid orbitals, whereas the CB consists of Bi 6p. It has been found that the broad VB increases the mobility of the photogenerated carriers⁽¹⁴⁾. This phenomenon is obvious for the bismuth-based photocatalysts because the Bi 6s orbital is largely dispersed, which is more beneficial to increasing the mobility of photogenerated carriers. Additionally, it was reported⁽¹⁵⁾ that the Bi-O sites in Bi³⁺-doped TiO₂ acted as electron traps in the photocatalytic reaction. As a consequence, materials containing Bi are probably active photocatalysts. The aim of the study is to prepare (BiOX, X = Cl, Br, I) and identified it by using FT-IR, X-ray diffraction (XRD) and scanning electron microscopy (SEM), then study its photocatalytic properties by changing the effect of catalyst weight, pH, temperature and initial concentration of the used dye.

2. Experimental

2. 1. Preparation of BiOX

Bismuth oxyhalide (BiOX, X = Cl, Br, and I) powders were synthesized using the hydrolysis method. Bi₂O₃ was dissolved in excessive concentrated halogen acid to obtain a BiX₃-HX aqueous system. A white precipitates appeared when the pH value of the solution was adjusted to about pH= 2 with ammonia. Then the precipitates were purified by filtration and washed with distilled water several times and heated at 100°C to dryness, powdery white BiOCl, yellowish BiOBr, and brick red BiOI were obtained.

As shown in the following equations. (1) and (2) (X = Cl, Br, and I):



2.2. Photoreactor

Photocatalytic degradation experiments were carried out in a 250 ml Pyrex-glass cell in the UV chamber 6W having a wavelength of 245 nm. Magnetic stirrer was used to ensure uniform mixing of solution in vessel. Before irradiation the dispersions were magnetically stirred in dark for 15 min to ensure the establishment of adsorption/desorption equilibrium.

2.3 Irradiation experiments

A photocatalyst was added to 100 mL of dye solution and the solution was irradiated under UV light. Then a little of the solution was withdrawn and filtered at different time. Absorption spectra of the dye solutions were recorded and rate of decolorization was observed in terms of change in intensity at λ_{\max} of the dye.

The decolorization efficiency (%) has been calculated as:

$$R = ((C_o - C_e) / C_o) \times 100 \quad (3)$$

3. Results and discussion

3.1. Characterization of prepared BiOX

3.1.1 FT-IR spectrum

The FT-IR spectra of the prepared catalysts were recorded using the FT-IR-8400S as a potassium bromide disc in the region (400 - 4000 cm^{-1}) at room temperature. Where a group of vibrational frequencies of the main bands appear in the spectra of the catalysts and indicate the formation of the catalytic compounds. In BiOCl we notice two characteristic bands was appeared at (1600-1620.26) cm^{-1} due to water, and at 528.51 cm^{-1} , 516.94 cm^{-1} , 486.08 cm^{-1} due to BiOCl⁽¹⁰⁾, BiOBr and BiOI⁽¹⁶⁾ respectively.

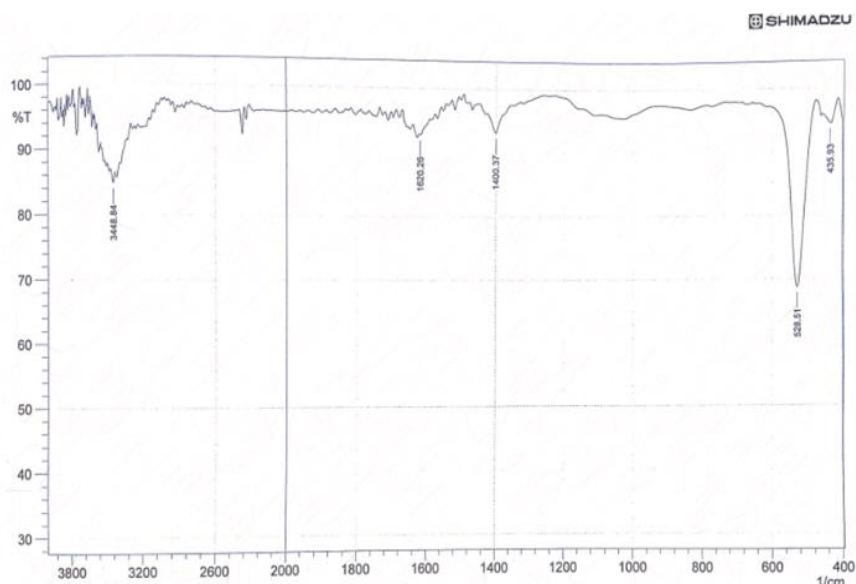


Figure (3.1) FT-IR spectrum of BiOCl

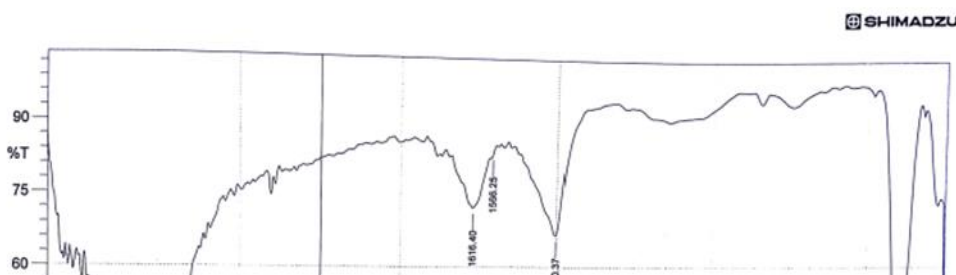


Figure (3.3) FT-IR spectrum of BiOBr

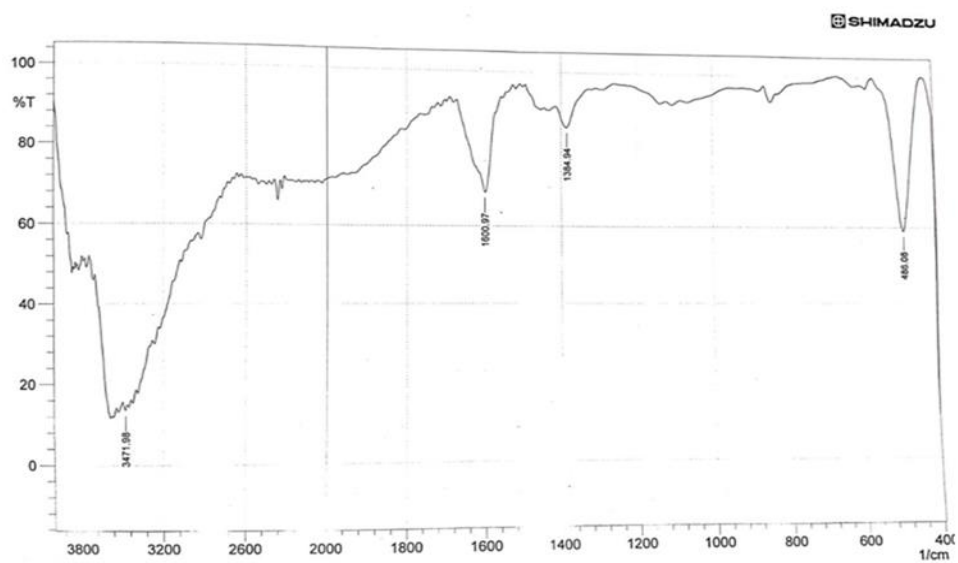


Figure (3.2) FT-IR spectrum of BiOI

3.1.2 X-Ray diffraction

It is one of the analytical techniques that gives information about the crystal structure, chemical composition and physical properties of materials. In this study, the XRD measurement of the prepared catalysts surfaces was taken before the adsorption process. XRD pattern of bismuth oxyhalide shows peaks at:

$$[^\circ 2\text{Th.}] \text{ of BiOCl} = (25.5)^\circ \text{A}.$$

$$[^\circ 2\text{Th.}] \text{ of BiOBr} = (32.5)^\circ \text{A}.$$

$$[^\circ 2\text{Th.}] \text{ of BiOI} = (30)^\circ \text{A}.$$

that confirm the tetragonal crystal structure of them. An increase in the ionic radii of X (from Cl to I), the XRD peaks shifted toward a smaller angle, and the lattice parameters increased slight⁽⁹⁾.

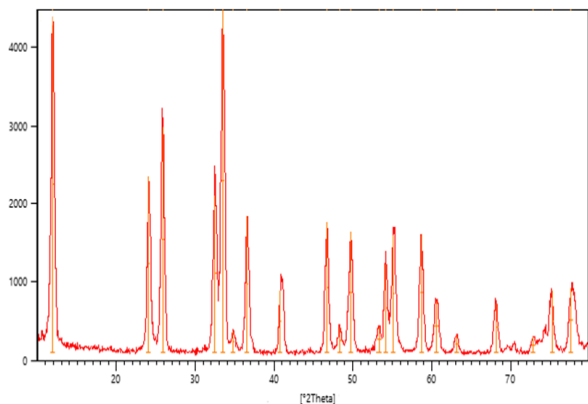


Figure (3.4) XRD spectrum of BiOCl

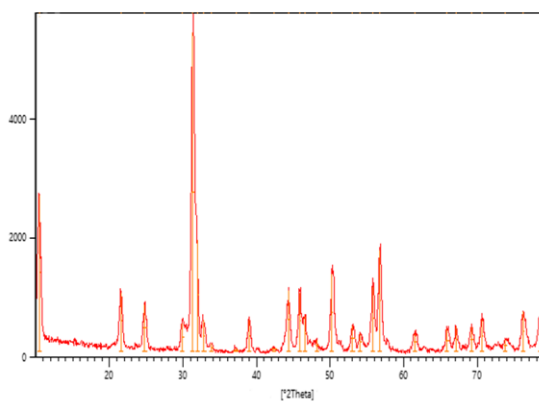


Figure (3.5) XRD spectrum of BiOBr

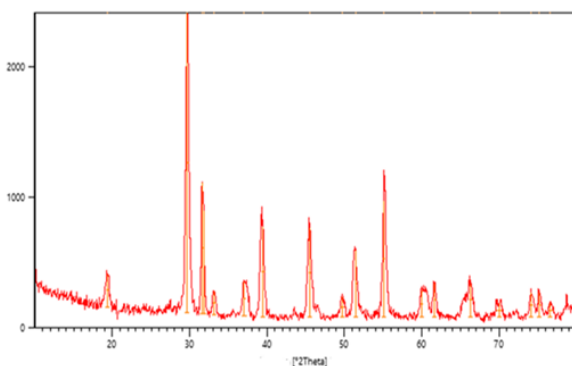


Figure (3.6) XRD spectrum of BiOI

3.1.3 Scanning Electron Microscopy (SEM)

Electron scanning of the prepared surfaces was taken before the adsorption process. Electron scanning was taken using a scanning electron microscope, a type of electron microscope that gives pictures of the sample by scanning the sample with a focused beam of electrons. The electrons interact with the sample atoms and give different signals containing information and surface terrain. Images SEM of the samples shown in Fig.(3.7), (3.8), (3.9) display the homogeneous sheet-shaped BiOX crystals with a thickness of about 100 nm. Sizes crystallite were in the range of several hundred nanometers to a few micrometers. Increase in the ionic radii of X (from Cl to I), the particles got thinner and their surfaces became larger, which were beneficial for their adsorption of the dye molecule⁽⁹⁾.

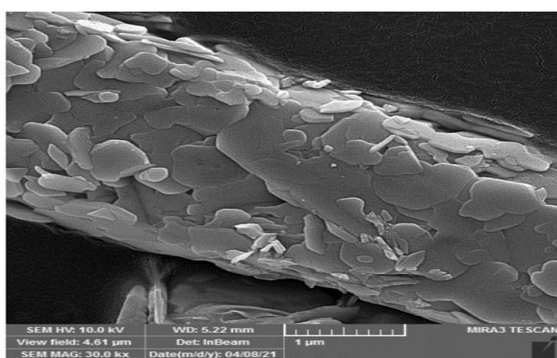


Figure (3.7) SEM of BiOCl

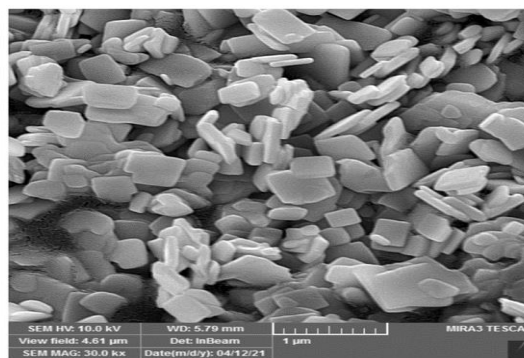


Figure (3.8) SEM of BiOBr

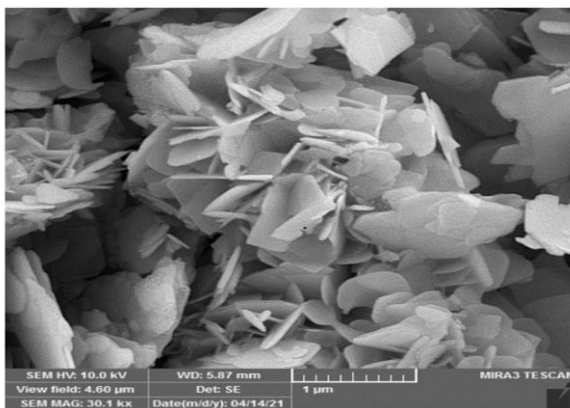


Figure (3.9) SEM of BiOI

3.2 Energy Dispersive X-rays Analysis (EDX)

It is an analytical technique used in order to analyze the elements to know the chemical properties of the sample. This occurs by bombarding the material with a beam of electrons, as in scanning electron microscopy, or with a beam of X-rays, as in XRD analysis. Figures (3.10), (3.11), (3.12) show the X-ray analysis spectra of the prepared compounds, and the table (3.1) shows the percentages of the abundance of the compounds.

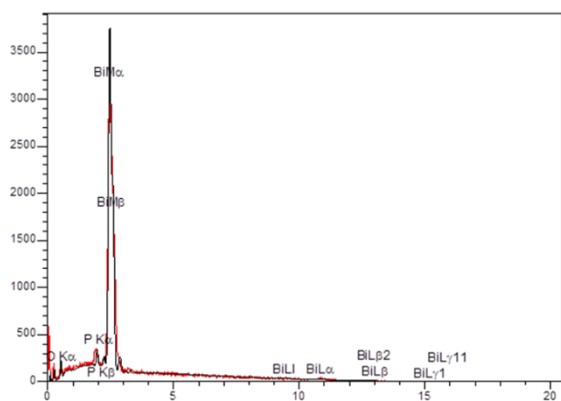


Figure (3.10) EDX of BiOCl

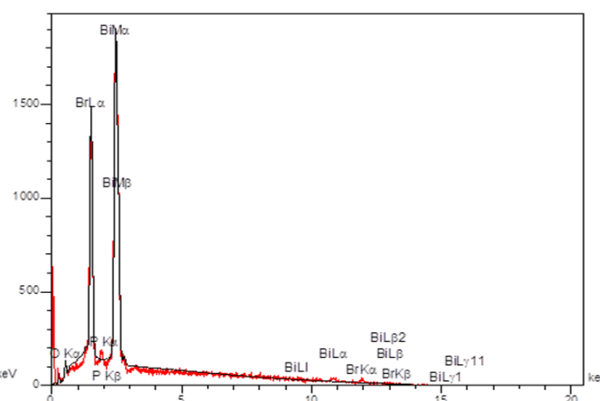


Figure (3.11) EDX of BiOBr

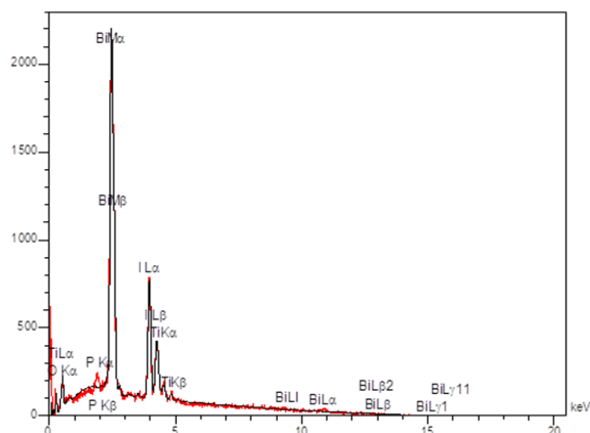


Figure (3.12) EDX of BiOI

Element %					Comp
I	Br	Cl	O	Bi	
-	-	3.71	5.67	89.67	BiOCl
-	22.74	-	4.78	69.62	BiOBr
29.13	-	-	5.73	45.11	BiOI

Table (3.1) percentages of the abundance of the compounds in EDX.

3.3. Degradation of Indigo carmine by BiOX

3.3.1. Effect of BiOX weight

In photocatalytic processes, the amount of catalyst is very important, the percentage change of dye removal with changing weights of the catalyst was studied by taking different weights of the catalyst, which are (0.06, 0.1, 0.2, 0.3 gm) concentration of 25mg/L, and a volume of 100 ml of indigo carmine dye solution (IC). The results were as shown in graph (3.10). Most of the results indicate an increase in the percentage with an increase in the weight of the catalyst due to the increase in the surface area and the availability of more active sites (which remain unsaturated due

to the increase in the surface weight for the dye molecules that remain stable) that are prepared to absorb the dye⁽¹⁷⁾ Any adsorption sites remain unsaturated during the catalytic process, as the adsorption sites increase with the increase in the surface area of the catalyst. A weight of 0.2 gm was constant and the effect of the pH, temperature and the initial concentration of the dye was studied.

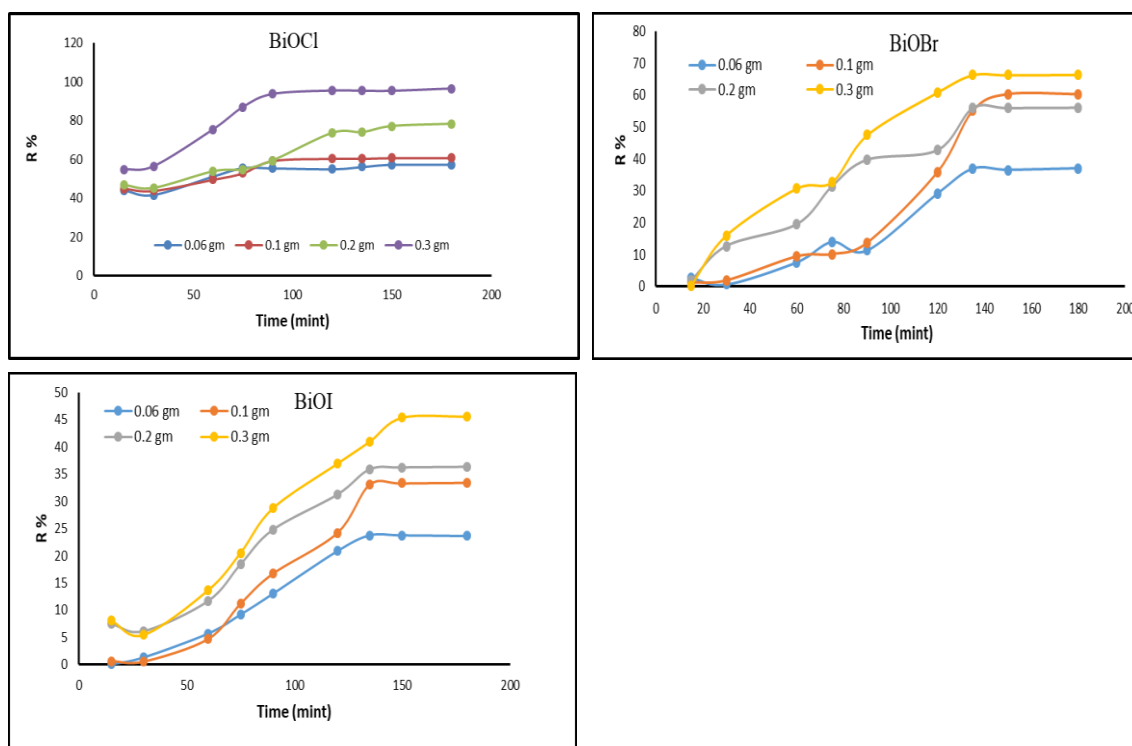


Figure (3.13) Effect of catalyst weight on the degradation of (IC) dye

3.3.2. Effect of pH

Photocatalytic process efficiencies depends on the acidity function of the reaction solution, where a range of pH (3,7,10) was taken at laboratory temperature and monitored over multiple times.

Degradation rate of dye clear at pH(10), meaning the dye's ability to bond with the surface is more than its tendency to bond with solvent molecules⁽¹⁸⁾. The removal of dye in photocatalysis is subject to various mechanisms such as direct reduction via electrons in the conduction band, direct oxidation through gaps in the valence band, and finally hydroxyl radical attack. The degree of contribution of each mechanism depends on the nature of the substance and the pH⁽¹⁹⁾. The pH is capable of modifying the electrical double layer of the liquid-solid interface and can affect the adsorption and desorption process thus hampering the electron-gap recombination process⁽¹⁰⁾.

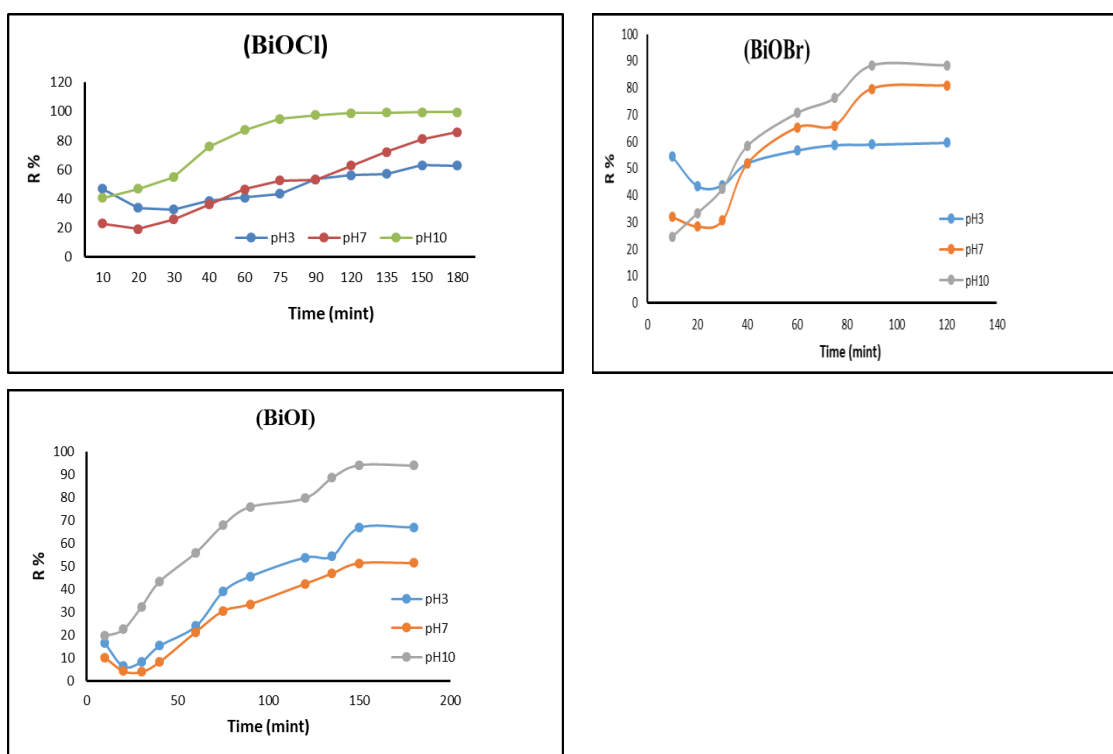


Figure (3.14) Effect of pH on the degradation of (IC) dye

3.3.3. Effect of Temperature

The effect of temperature on the catalytic process was studied using two different temperatures, namely (50 and 60 °C) compare with room temperature, where it is noted that the degradation increases with increasing

temperature with the time of (BiOBr, BiOI). The increase in the removal rate is due to occurrence of an absorption process in addition to adsorption that meaning occurs chemical adsorption. An increase in temperature increases the spread of adsorbed molecules on the surface within the pores on the adsorbent surface⁽²⁰⁾.

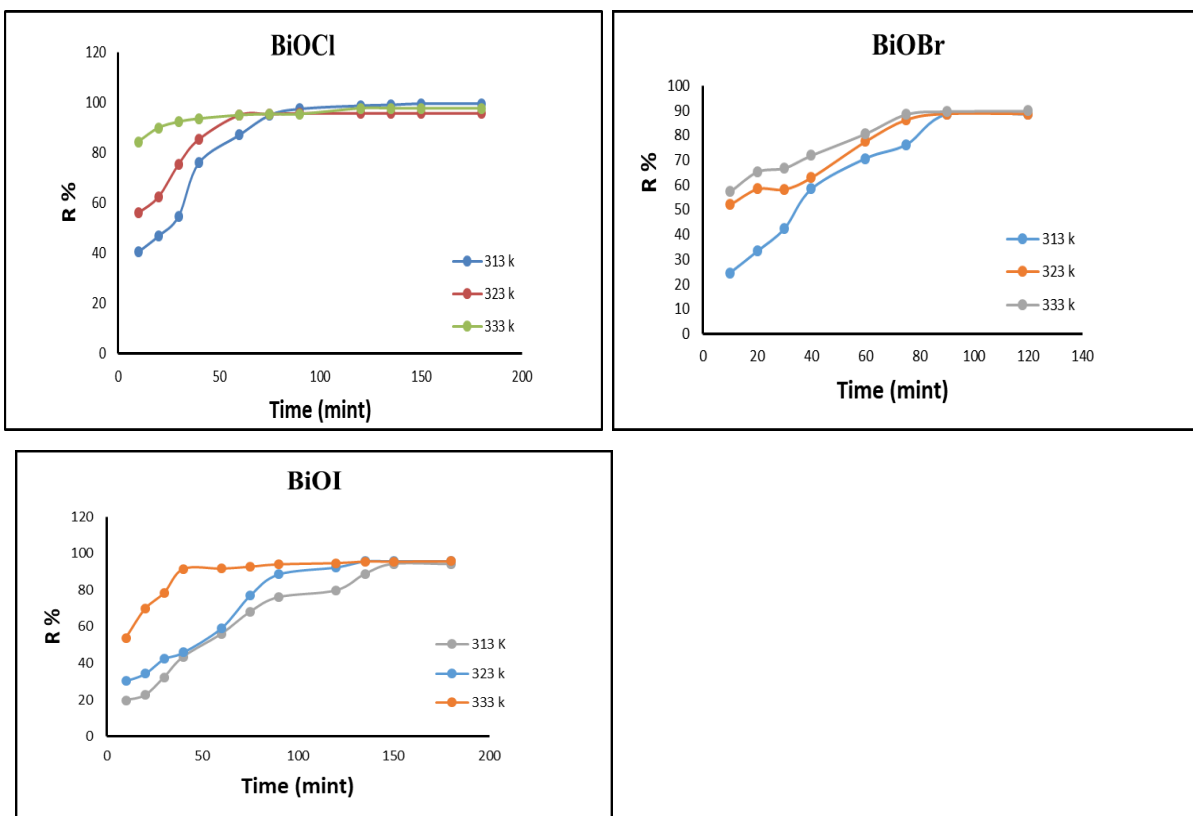


Figure (3.15) Effect of temperature on the degradation of (IC) dye

3.3.4. Effect of initial concentration dye

The effect of the initial concentration of the dye is an important aspect of the study, the initial concentrations varied within the range of (20-100) mg/L. The rate of decomposition decreased with the increase in the initial concentration of the dye solution over time, as more organic matter (dye) was adsorbed on the surface of the catalyst compounds (BiOCl, BiOBr, BiOI), so the production of hydroxyl radicals would be reduced due to the presence of fewer active sites for the adsorption of hydroxyl ions and generation of hydroxyl radicals. Furthermore, increasing the concentration of the dye solution traps the photons before they reach the surface of the catalyst, thus decreasing the absorption of the photons, thus reducing the rate of degradation⁽²¹⁻²³⁾.

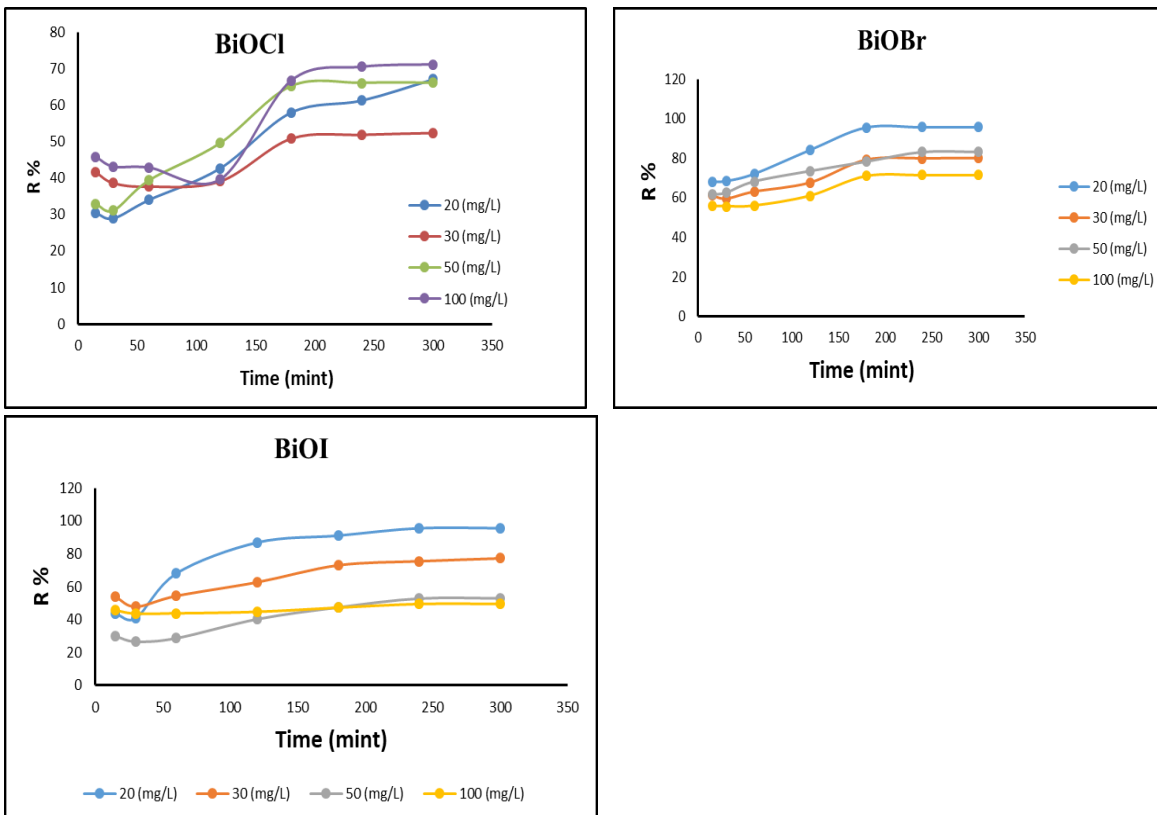


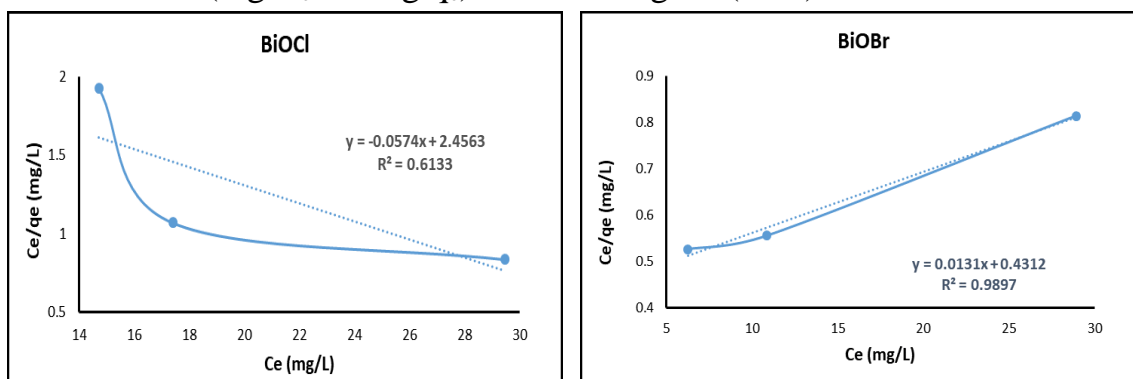
Figure (3.16) Effect of the initial concentration of the (IC) dye

3.4. Adsorption Isotherm

The adsorption isotherm was studied by applying the Langumire and Freundlich equation⁽²⁴⁾ using different concentrations and one temperature. And from the data of the isotherms shown in figure (3.17).

The Langumire constant (K_L), the maximum adsorption value (Q_m), and the correlation coefficient (R^2) were calculated and these values are shown in a table (3.2).

The linear relationship of the Freundlich equation was also drawn based on the values of ($\log C_e$ vs. $\log q_e$) shown in figure (3.18).



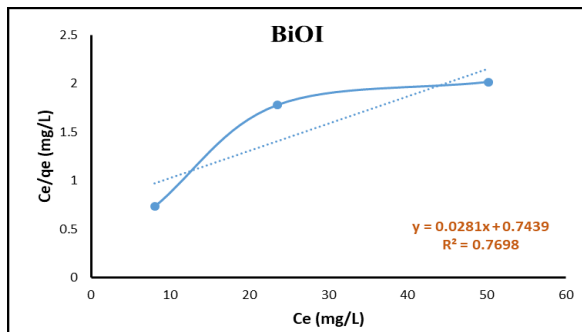


Figure (3.17) Langmuire isotherm for adsorption of (IC) dye

Comp	Temp	Q_m	K_L	R^2
BiOCl	50 °C	-17.42160	-0.02336	0.6133
BiOBr	50 °C	76.33587	0.030380	0.9897
BiOI	50 °C	35.58718	0.02090	0.7698

Table (3.2) values of Langmuire constants for adsorption of dye on the surfaces of compounds (BiOCl, BiOBr, BiOI) at one temperature

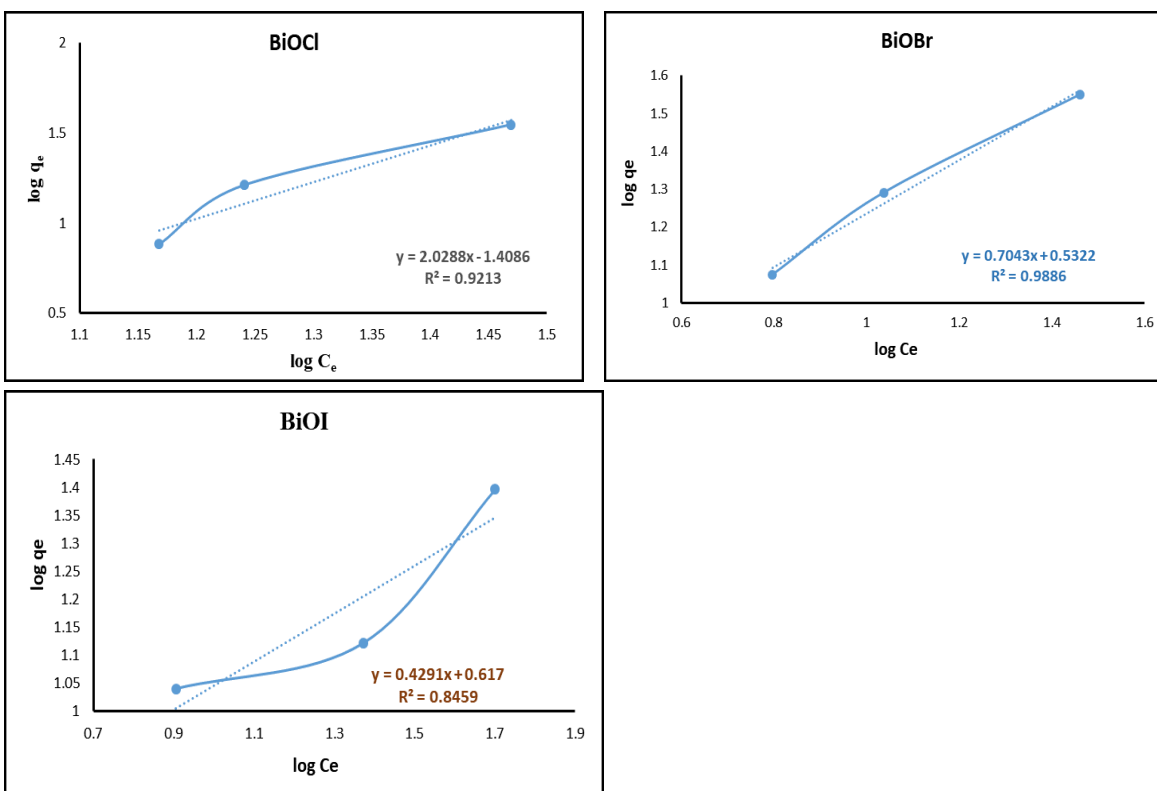


Figure (3.18) Linear relationship of the Freundlich isotherm for (IC) dye adsorption

Comp	Temp	n	K_f (1/mg)	R^2
BiOCl	50 °C	0.492902208	4.0902250	0.9213
BiOBr	50 °C	1.419849496	1.7026740	0.9886
BiOI	50 °C	2.3304591	1.8533596	0.8459

Table (3.3) values of Freundlich constants for adsorption of dye on (BiOCl, BiOBr, BiOI) at one temperature

From the results shown in the tables (3.4), (3.5) we conclude that reactions of (BiOCl, BiOI) are subject to the Freundlich equation. While BiOBr is subject to the Langmuir equation.

3.5. Thermodynamic study

The study of the effect of temperature helps to estimate the values of the thermodynamic functions represented by enthalpy (ΔH), entropy (ΔS), free energy (ΔG).

The figures (3.24), (3.25), (3.26) show the linear relationship of $\ln K$ values versus $1/T$ values for dye adsorption on the surfaces of catalytic compounds. The values of the thermodynamic functions are shown in the table (3.7).

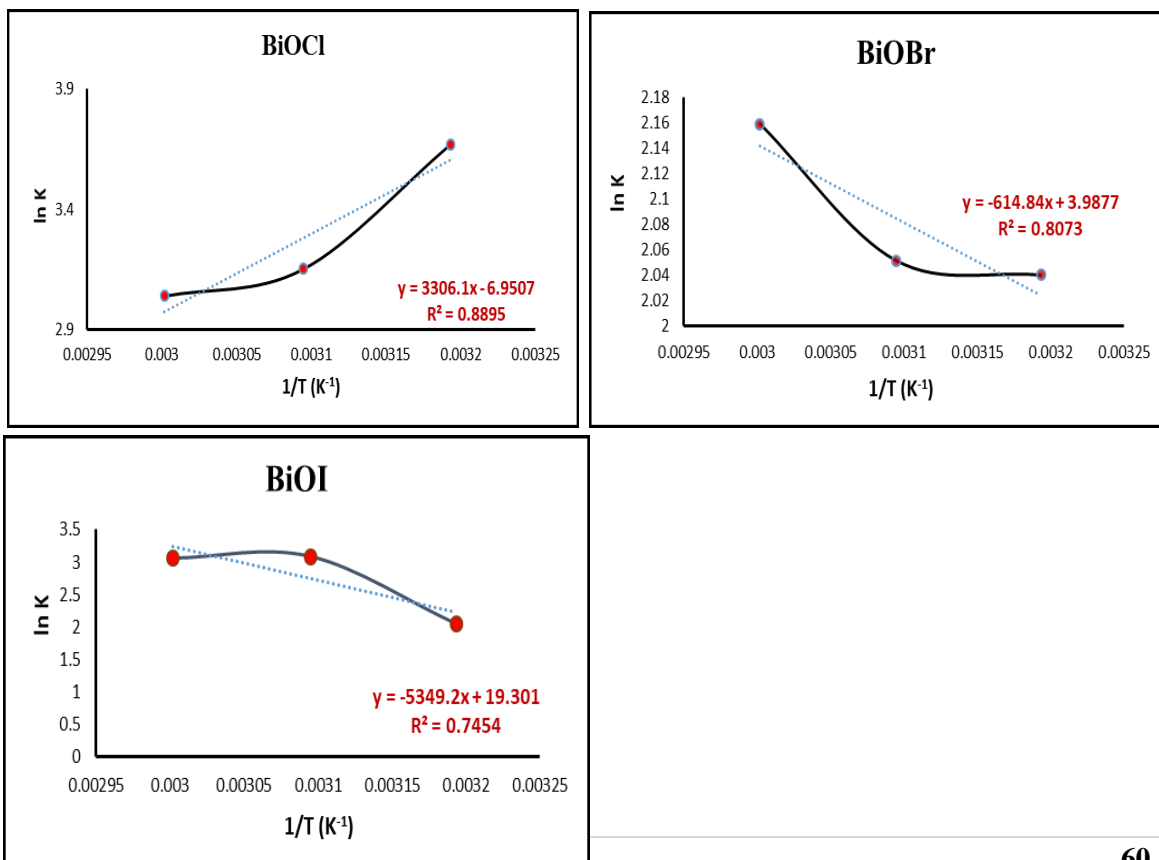


Figure (3.19) the linear relationship between the values of $\ln K$ versus $1/T$ for adsorption of (IC) dye

Comp	ΔG (KJ.mol ⁻¹)			ΔH (KJ.mol ⁻¹)	ΔS J.mol ⁻¹ K ⁻¹
	40°C	50°C	60°C		
BiOCl	-45.583	-46.161	-46.739	-27.486	57.788
BiOBr	-5.270	-5.601	-5.933	5.111	33.153
BiOI	-5.779	-7.383	-8.988	44.471	160.468

Table (3.4) values of thermodynamic functions for adsorption of dye on (BiOCl, BiOBr, BiOI) at different temperatures and 25mg/L.

3.5.1. Explanation of Table (3.4)

1. The value of the heat of adsorption (ΔH) for (BiOBr, BiOI) positive values, meaning that the adsorption process is endothermic, and this indicates the presence of an adsorption process as well as an adsorption process, meaning that with an increase in temperature, the speed of diffusion of the adsorbed molecules on the adsorbent surface increases within the pores on the surface⁽²⁵⁾. Heat of adsorption (ΔH) for (BiOCl) negative value in the sense that the adsorption process is of the exothermic type. This means that the speed of propagation of the adsorbed molecules on the surface decreases with the increase in temperature. Therefore, the reciprocal action between the adsorbent molecules and the adsorbing surface decreases⁽²⁶⁾ as the increase in temperature leads to an increase in the kinetic energy of the adsorbed molecules on the surface This increases the possibility of its separation from the adsorbent surface and back into the solution.

2. The entropy (ΔS) value for catalysts adsorption are positive, meaning that the adsorbed molecules are still in a state of continuous movement on the adsorbent surface, which is attributed to the occurrence of an adsorption process as well as an adsorption process⁽²⁷⁾.

3. The value of free energy (ΔG) for this catalysts adsorption is negative, meaning that the adsorption process is spontaneous.

3.6 Kinetic Study

The adsorption kinetics of the dye on the surfaces of the prepared compounds was studied by applying the following two equations:

1. The pseudo first-order equation: it is called Lagergren. This equation can be expressed by the following formula⁽²⁸⁾:

$$\ln (q_e - q_t) = \ln q_e - k_1 t \dots\dots\dots (4)$$

2. pseudo second order equation: This equation can be expressed by the following formula^(29,30):

$$t/(q_t) = 1/(k_2 q_e^2) + 1/q_t t \dots\dots\dots (5)$$

The effect of temperature differences on the adsorption kinetics of the bismuth oxyhalide prepared at temperatures (40, 50, 60) °C, fixed volume (100 ml), concentration (25 mg/L) and constant weight (0.2 gm) and at different times until the special equilibrium time was studied.

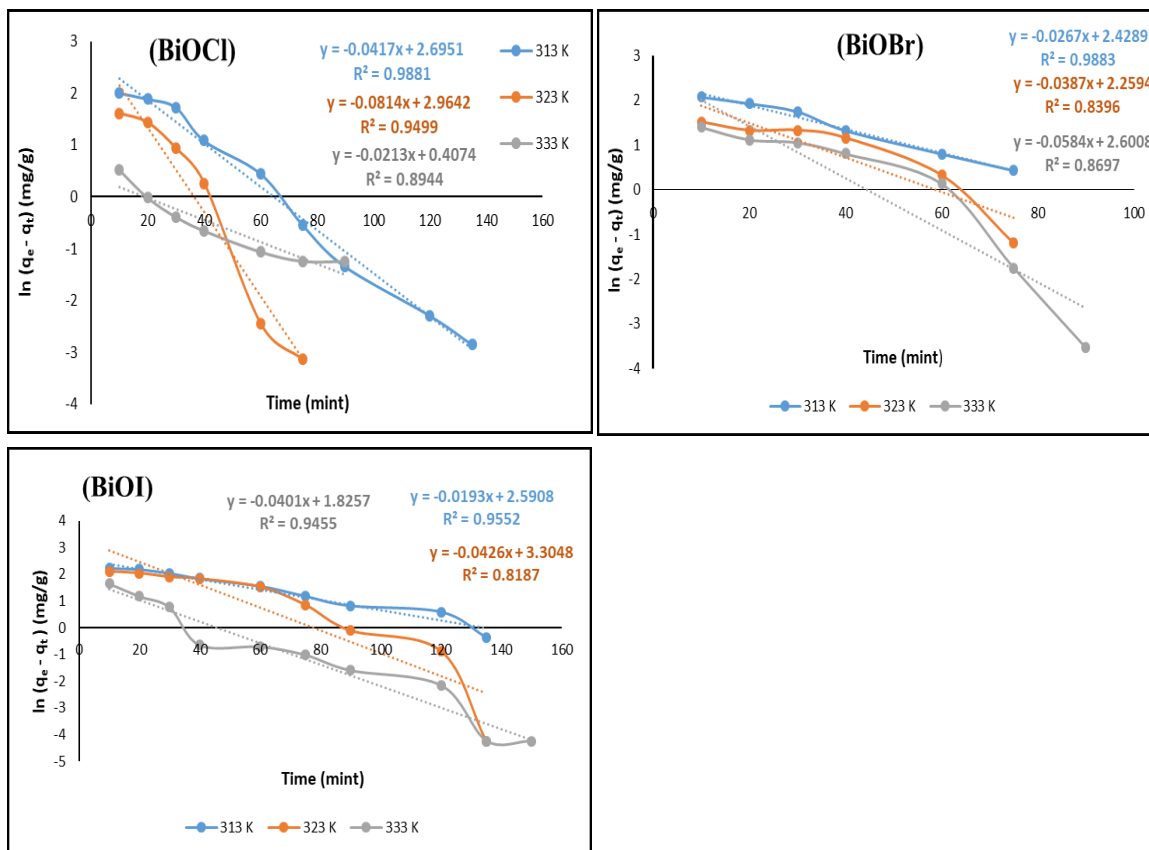


Fig. (3.20) Linear relationship of Lagergren equation for adsorption of (IC) dye

Comp	Temp _k	q _e (exp) (mg/g)	q _e (cal) (mg/g)	K ₁ (mint ⁻¹)	R ²
BiOCl	313	12.4494	14.8069	0.0417	0.9881
	323	11.9869	19.3791	0.0814	0.9499
	333	12.2182	1.50290	0.0213	0.8944
BiOBr	313	11.0621	11.34639	0.0267	0.9883
	323	11.0765	9.57734	0.0387	0.8396
	333	11.2355	13.47451	0.0584	0.8697
BiOI	313	11.7702	13.34043	0.0193	0.9552
	323	11.9725	27.24309	0.0426	0.8187
	333	11.9580	6.20713	0.0401	0.9455

Table (3.5) values of the adsorption rate constant K₁ and the experimental and calculated adsorption capacity q_e(cal), q_e(exp) for the pseudo-first-order equation

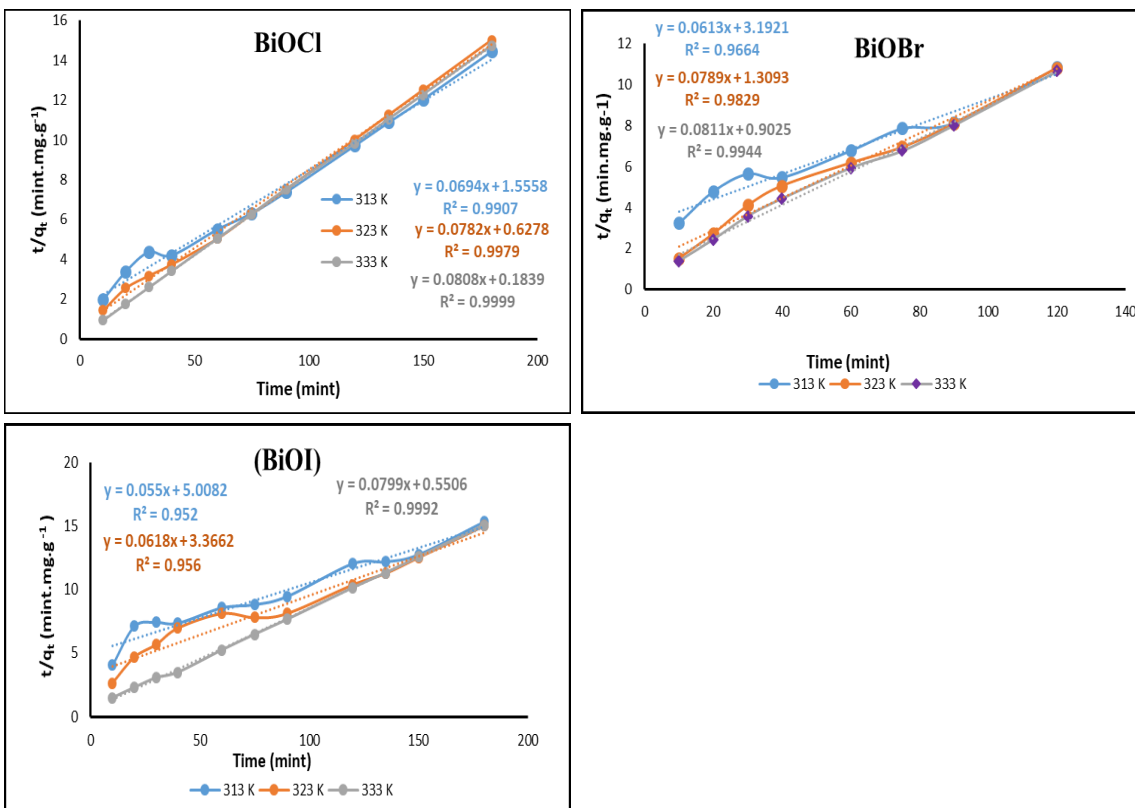


Figure (3.21) Linear relationship of the pseudo second-order equation for adsorption of (IC) dye

Comp	Temp K	$q_e(\text{exp})$ (mg/g)	$q_e(\text{cal})$ (mg/g)	K_2 (mint^{-1})	R^2
BiOCl	313	12.4494	14.409	0.007493	0.9907
	323	11.9869	13.297	0.004439	0.9958
	333	12.2182	12.330	0.001120	0.9998
BiOBr	313	11.0621	16.313	0.011994	0.9664
	323	11.0765	12.674	0.008150	0.9829
	333	11.2355	12.330	0.005935	0.9944
BiOI	313	11.7702	18.181	0.015149	0.952
	323	11.9725	16.181	0.012856	0.956
	333	11.9580	12.515	0.003515	0.9992

Table (3.5) values of the adsorption rate constant K_2 and the experimental and calculated adsorption capacity $q_e(\text{cal})$, $q_e(\text{exp})$ for the pseudo-second order equation for adsorption of (IC) dye on the catalysts.

From the tables (3.4) and (3.5) we notice that the values of the empirical adsorption capacity ($q_e(\text{exp})$) and the calculated adsorption capacity ($q_e(\text{cal})$) at equilibrium for the pseudo first-order equation are not identical as the difference between them is large, but we note that these values are close to some of them to the equation of the pseudo second order. Also, when comparing the values of the correlation coefficient R^2 in both tables, we notice that the pseudo second-order equation correlation coefficient is greater than the pseudo first-order correlation coefficient, so the pseudo second-order adsorption kinetics equation is more identical than the pseudo first-order equation. That meaning all of compounds subject to pseudo second-order.

Conclusion:

New series of photocatalysts, bismuth oxyhalide (BiOX, X = Cl, Br, and I), were synthesized by the hydrolysis method. SEM pattern showed that all the BiOX are homogeneous crystals in the form of sheets. As the ionic radius of (X) increased from Cl to I, the particles became thinner and their surface larger than was useful for adsorbing dye molecules. EDX pattern showed the percentages of abundance of the elements were very good, which indicates the formation of these compounds. The pH had a clear effect on the removal

rate. Heat of adsorption of BiOCl is exothermic and BiOBr, BiOI are endothermic. All of this catalysts subject to pseudo second-order.

References:

1. Arakawa, H. *et al* (2001): Catalysis research of relevance to carbon management: Progress, challenges, and opportunities. *Chem. Rev.* **101**, 953–996.
2. Esswein, A. J. & Nocera, D. G. (2007): Hydrogen production by molecular photocatalysis. *Chem. Rev.* **107**, 4022–4047.
3. Haji-Saeid, S. M., Sampa, M. H., Safrany, A., Sabharwal, S. & Ramamoorthy, N. (2012): Radiation processing techniques in remediation of pollutants, and the role of the IAEA in supporting capacity building in developing countries. *Radiat. Phys. Chem.* **81**, 1040–1044.
4. Hashim, M. A., Mukhopadhyay, S., Sahu, J. N. & Sengupta, B. (2011): Remediation technologies for heavy metal contaminated groundwater. *J. Environ. Manage.* **92**, 2355–2388.
5. Yeung, A. T. & Gu, Y. Y. (2011): A review on techniques to enhance electrochemical remediation of contaminated soils. *J. Hazard. Mater.* **195**, 11–29.
6. Khan, F. I., Husain, T. & Hejazi, R. (2004): An overview and analysis of site remediation technologies. *J. Environ. Manage.* **71**, 95–122.
7. Finegold, L. & Cude, J. L. (1972): Biological sciences: One and two-dimensional structure of alpha-helix and beta-sheet forms of poly(L-Alanine) shown by specific heat measurements at low temperatures (1.5-20 K). *Nature* **238**, 38–40.
8. Hoffmann, M. R., Martin, S. T., Choi, W. & Bahnemann, D. W. (1995): Environmental Applications of Semiconductor Photocatalysis. *Chem. Rev.* **95**, 69–96.
9. AN, H. *et al.* (2008): Photocatalytic properties of BiOX (X = Cl, Br, and I). *Rare Met.* **27**, 243–250.
10. ElShafei, G. M. S. *et al.* (2018): Metal oxychlorides as robust heterogeneous Fenton catalysts for the sonophotocatalytic degradation of 2-nitrophenol. *Appl. Catal. B Environ.* **224**, 681–691.
11. Zhang, K. L., Liu, C. M., Huang, F. Q., Zheng, C. & Wang, W.

- D.(2006): Study of the electronic structure and photocatalytic activity of the BiOCl photocatalyst. *Appl. Catal. B Environ.* **68**, 125–129.
12. Zhang, L. *et al.* (2006): Sonochemical synthesis of nanocrystallite Bi₂O₃ as a visible-light-driven photocatalyst. *Appl. Catal. A Gen.* **308**, 105–110.
 13. Tang, J., Zou, Z. & Ye, J. (2004): Photocatalytic decomposition of organic contaminants by Bi₂WO₆ under visible light irradiation. *Catal. Letters* **92**, 53–56.
 14. He, C. & Gu, M. (2006): Photocatalytic activity of bismuth germanate Bi₁₂GeO₂₀ powders. *Scr. Mater.* **54**, 1221–1225 (2006).
 15. Rengaraj, S., Li, X. Z., Tanner, P. A., Pan, Z. F. & Pang, G. K. H. Photocatalytic degradation of methylparathion - An endocrine disruptor by Bi³⁺-doped TiO₂. *J. Mol. Catal. A Chem.* **247**, 36–43.
 16. Wang, Y., Deng, K. & Zhang, L. (2011): Visible light photocatalysis of BiOI and its photocatalytic activity enhancement by in situ ionic liquid modification. *J. Phys. Chem. C* **115**, 14300–14308.
 17. Elywe, A. H. (2013): Adsorption equilibria of methylen blue dye from aqueous Ayad Fadhil Alkaim Corresponding author : ayad_alkaim@yahoo.com. **51**, 301–315.
 18. Radhi, I. K., Hussein, M. A. & Kadhim, Z. N. (2019): Factors Affecting the Adsorption of Some Ionic Dyes on the Surface of Modify CaO from Eggshell. *Asian J. Appl. Sci.* **7**,.
 19. Tang, W. Z., Zhang, Z., An, H., Quintana, M. O. & Torres, D. F. (1997): TiO₂/uv photodegradation of azo dyes in aqueous solutions. *Environ. Technol. (United Kingdom)* **18**, 1–12.
 20. Langmuir, I. (1917): The constitution and fundamental properties of solids and liquids. Part II.-Liquids. *J. Franklin Inst.* **184**, 721.
 21. Qamar, M., Saquib, M. & Muneer, M. (2005): Photocatalytic degradation of two selected dye derivatives, chromotrope 2B and amido black 10B, in aqueous suspensions of titanium dioxide. *Dye. Pigment.* **65**, 1–9.
 22. Daneshvar, N., Rabbani, M., Modirshahla, N. & Behnajady, M. A. (2004): Kinetic modeling of photocatalytic degradation of Acid Red 27 in UV/TiO₂ process. *J. Photochem. Photobiol. A Chem.* **168**, 39–

- 45.
23. Wu, C. H. (2004): Comparison of azo dye degradation efficiency using UV/single semiconductor and UV/coupled semiconductor systems. *Chemosphere* **57**, 601–608.
 24. Jaafar, J. S., Abdulwahid, A. A. & Maarch, Y. A. (2021): Preparation and characterization of some esters impregnated with magnetic iron oxide nanoparticles Fe₃O₄ and study of their efficiency in for adsorption of lead ions from their aqueous solutions. **39**.
 25. Ahmad, M. A., Ahmad Puad, N. A. & Bello, O. S. (2014): Kinetic, equilibrium and thermodynamic studies of synthetic dye removal using pomegranate peel activated carbon prepared by microwave-induced KOH activation. *Water Resour. Ind.* **6**, 18–35.
 26. Sawasdee, S. & Watcharabundit, P. (2015): Equilibrium, Kinetics and Thermodynamic of Dye Adsorption by Low — Cost Adsorbents. *Int. J. Chem. Eng. Appl.* **6**, 444–449.
 27. Branton, P. J. *et al.* (1994): Physisorption of argon, nitrogen and oxygen by MCM-41, a model mesoporous adsorbent. *J. Chem. Soc. Faraday Trans.* **90**, 2965–2967.
 28. Almalike, L. B., Al-najar, A. A. & Kadhim, Z. N. (2016): Physical characteristics of adsorption – desorption of Fipronil in the soil. **4**, 26–35.
 29. Hussein, M. A. & Kadhim, Z. N. (2019): Eur opean J ournal of Chem istry. **2249**, 64–71.
 30. Kadhim, Z. N. (2016): Using of Isolated Hydroxyapatite from Sheep Bones to Remove Lead (II) from Aqueous Solution and Studying the Thermodynamics and Adsorption Using of Isolated Hydroxyapatite from Sheep Bones to Remove Lead (II) from Aqueous Solution and Studying the The. *Asian J. Appl. Sci.* **04**, 149–160.